Highly localized sensitivity to climate forcing drives endemic cholera in a megacity

Robert C. Reiner, Jr.,[a,1,2], Aaron A. King[a,b], Michael Emch[c], Mohammad Yunus[d], A. S. G. Faruque[d], and Mercedes Pascual[a,e]

[a]Department of Ecology and Evolutionary Biology, University of Michigan, Ann Arbor, MI 48109; [b]Fogarty International Center, National Institutes of Health, Bethesda, MD 20892; [c]Department of Geography, University of North Carolina, Chapel Hill, NC 27599; [d]International Centre for Diarrheal Disease Research, Dhaka 1000, Bangladesh; and [e]Howard Hughes Medical Institute, Chevy Chase, MD 20815-6789

Edited by Ignacio Rodriguez-Iturbe, Princeton University, Princeton, NJ, and approved December 12, 2011 (received for review May 27, 2011)

The population dynamics of endemic cholera in urban environments—in particular interannual variation in the size and distribution of seasonal outbreaks—remain poorly understood and highly unpredictable. In part, this situation is due to the considerable demographic, socioeconomic, and environmental heterogeneity of large and growing urban centers. Despite this heterogeneity, the influence of climate variability on the population dynamics of infectious diseases is considered a large-scale, regional, phenomenon, and as such has been previously addressed for cholera only with temporal models that do not incorporate spatial structure. Here we show that a probabilistic spatial model can explain cholera dynamics in the megacity of Dhaka, Bangladesh, and afford a basis for cholera forecasts at lead times of 11 mo. Critically, we find that the action of climate variability (El Niño southern oscillation and flooding) is quite localized: There is a climate-sensitive urban core that acts to propagate risk to the rest of the city. The modeling framework presented here should be applicable to cholera in other cities, as well as to other infectious diseases in urban settings and other biological systems with spatiotemporal interactions.

risk propagation | cholera and flooding | disease forecasting | inhomogeneous Markov chain | spatiotemporal dynamics of urban cholera

In regions where cholera is endemic, the considerable year-to-year variation in the size of its seasonal outbreaks has motivated the development of models to retrospectively explain multiannual cycles in disease incidence and prospectively forecast the occurrence of large cholera events (1–3). Previous studies of endemic cholera have relied largely on data aggregated over relatively large spatial scales (2, 4, 5) and statistical models for recurrent outbreaks in urban centers have so far achieved prediction at lead times of ≤1 mo (6, 7), too short to be of use in early warning systems. Studies have also shown that the El Niño southern oscillation (ENSO) influences multiannual cycles in disease incidence (4, 2, 8, 9) but because such global climate drivers have been expected to act over large spatial scales and to synchronize epidemiological responses across space (the Moran effect) (10, 11) and because the physical and ecological linkages between global drivers and local transmission remain obscure (12–14, 16), the fine-scale spatiotemporal dynamics of endemic cholera have been largely ignored.

However, the rapid growth and pronounced demographic and socioeconomic heterogeneity of the emerging megacities of the modern era (17, 18) lead to significant fine-scale spatial structure with unexplored consequences for disease dynamics. In the case of fecal–oral diseases such as cholera, for which sanitary conditions and access to clean water are determinants of disease risk, heterogeneities on very local scales can be important, a fact that has been appreciated since Snow's mapping of the association between cholera risk and water contamination (19). On the other hand, a body of recent work has established a link between global climate drivers—in particular the ENSO—and cholera dynamics. The existence of key predictors on these two vastly different scales begs the following questions: (*i*) What linkages mediate the action of global climate drivers at the local scale? (*ii*) Can we combine data at these two scales to obtain a useful cholera early-warning system?

We formulated a probabilistic model for cholera dynamics within the city of Dhaka and fit it to O1 El Tor cholera hospitalization data broken down into administrative subdivisions called *thanas* (Fig. 1). The monthly data span the period 1995–2008 and include all cases since the last disappearance of the O1 classical and O139 strains. The cholera case data used here were collected by International Centre for Diarrhoeal Disease Research, Bangladesh (ICDDR,B) hospital located in Dhaka city. This hospital provides free treatment to ∼110,000 diarrhea cases annually. A systematic 4% sample (every 25th patient) from 1984 to 1995 and 2% sample (every 50th patient) from 1996 onward were taken from all patients that reported to Dhaka hospital irrespective of disease severity. Fecal specimens were collected from these patients and were cultured for diagnosis of cholera following standard procedures. Inspection of the data suggested the existence of two distinct regions within Dhaka: one comprising the older core districts and the other, the newer urban periphery (Fig. 1). Cholera attack rates in the core districts are higher than in the periphery (Fig. 2 *B* and *C* and Movie S1).

Our model assigns a probability to transitions in cholera rate for each thana each month. We categorize the cholera attack rate in each thana into "no cholera," "low cholera," and "high cholera," using a criterion described in *section S1*. The model is thus a finite-state Markov chain (20, 21). We allow the transition probabilities to depend on temporal and spatial covariates as well as the state of neighboring thanas. Because all thanas' transitions must be considered simultaneously, the model is a multidimensional inhomogeneous Markov chain (MDIMC), schematized in Fig. 3. Each month, each thana is in one of three states. In the next month, each thana probabilistically changes its state according to transition probabilities that depend on temporal and spatial covariates as well as the state of neighboring thanas. We enforced the total-probability constraint through choice of parameterization and use of the "barrier method"; we verified that the conclusions summarized below are all robust to alternative parameterization (see *section S2* and *section S3* for a description of the barrier method and alternative parameterization analysis, respectively).

The model captures the inter- and intraannual dynamics of cholera in each thana. Likelihood-ratio tests can be used to test the

Author contributions: R.C.R., A.A.K., and M.P. designed research; R.C.R. performed research; R.C.R., A.A.K., M.E., M.Y., A.S.G.F., and M.P. analyzed data; and R.C.R., A.A.K., and M.P. wrote the paper.

The authors declare no conflict of interest.

This article is a PNAS Direct Submission.

Freely available online through the PNAS open access option.

[1]To whom correspondence should be addressed. E-mail: rcreiner@ucdavis.edu.

[2]Present addresses: Department of Entomology, University of California, Davis, Davis, CA, 95616; and Fogarty International Center, National Institutes of Health, Bethesda, MD 20892.

This article contains supporting information online at www.pnas.org/lookup/suppl/doi:10.1073/pnas.1108438109/-/DCSupplemental.

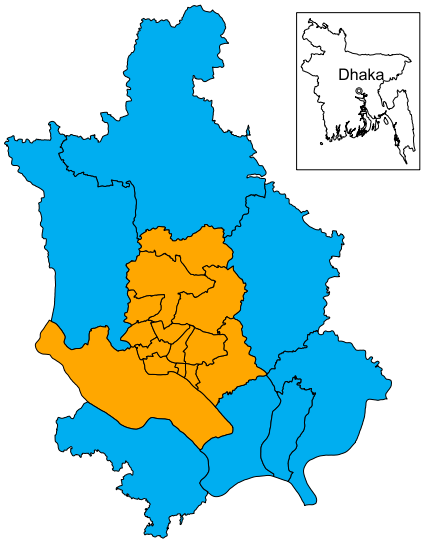

Fig. 1. The thanas (administrative subdivisions) of Dhaka. We divided thanas into two groups: older, core thanas (orange) and newer, peripheral thanas (blue).

statistical significance of covariates. Although binning the original numerical data into categories discards some information, it focuses attention on levels of variation that are relevant to public health. Comparison of the binned and original data shows that the percentiles of these two data sets match well and that loss of differentiation is present only for large outbreaks and rare extreme outbreaks (see Figs. S1 and S2 and Movie S2 for an animation of the binned data). A detailed description of the model and specific analyses performed can be found in *sections S2–S4*, Figs. S3–S5, and Tables S1 and S2.

We identified significant spatial effects at two different scales. The first effect corresponds to the core–periphery distinction shown in Fig. 1. Cholera transmission dynamics (as indicated by model transition matrices) differ significantly between core and peripheral thanas ($P < 0.0001$). The second effect is more local: We found a significant spatial effect between neighboring thanas ($P < 0.05$), implying propagation of outbreak risk from thana to thana.

The evidence for two distinct regions within the city raises the question of the interaction between climate forcing and the spatial dimension of disease dynamics. Consistent with previous studies for an earlier period (4, 8), we find that ENSO per se is a significant driver of cholera outbreaks in Dhaka ($P < 0.0001$). Warming in the Pacific precedes an effect on disease dynamics by 11 mo as indicated by the lag with highest likelihood. Importantly, we find a significantly greater effect of ENSO in the core relative to the periphery ($P < 0.05$). Thus, even though the city covers only 160 km^2, there is important heterogeneity in cholera's sensitivity to this global driver.

Previous studies of temporal cholera patterns have suggested that flooding may mediate the effect of ENSO locally (2, 22–24) via a dynamical linkage between sea surface temperature (SST) in the Pacific and regional precipitation in Bangladesh (16). Flooding events occur each summer in this region, vary in magnitude from year to year, and can be extensive in Dhaka. We identify a significant correlation between flooding and cholera cases both during and after the monsoon season ($P < 0.01$). We further investigated the interaction between the effect of flooding and region of the city and found the correlation varied

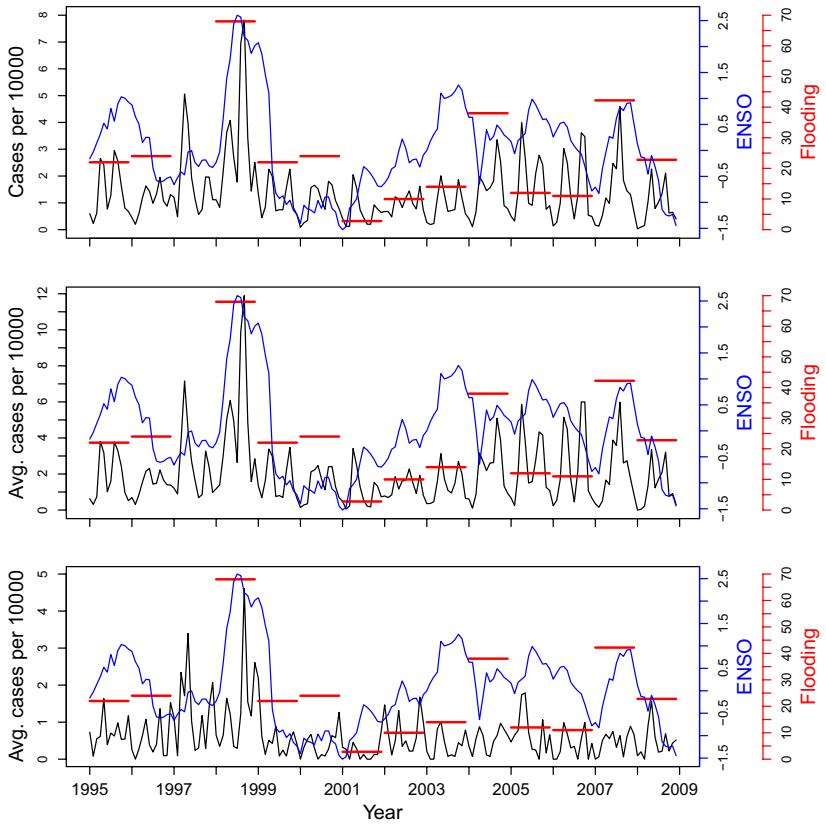

Fig. 2. Cases of cholera per 10,000 in Dhaka (in black) superimposed to an index for the El Niño southern oscillation (ENSO) (in blue) and annualized flood extent at the level of the country as a whole (red). (*Top*) The whole city of Dhaka; (*Middle*) the core, older region of the city; (*Bottom*) the peripheral, new regions. The interannual variability in the cholera rate is coherent with that of the climate covariates, especially for the older thanas and for the very large El Niño of 1998.

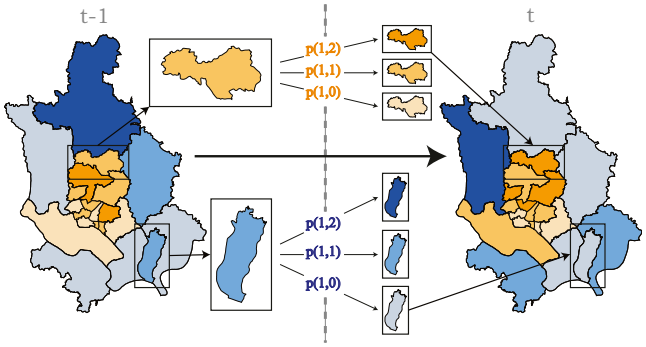

Fig. 3. Schematic representation of MDIMC model. Thanas of the same hue are governed by the same rules. Each thana can be in one of three states (0, 1, or 2 for no cholera, low cholera, or high cholera, respectively) as indicated by the different shades within each of the two groups. Probability of transitions between states from one month to the next can vary according to season, district group, state of neighboring districts, and climate covariates.

significantly spatially ($P < 0.01$). For example, flooding correlates strongly with the midmonsoon season cholera level within the core regions of the city ($r = 0.764$ for July), but is essentially uncorrelated within the peripheral regions ($r = -0.009$ for July). Moreover, in the 2 y with most extensive flooding—1998 and 2007—there was earlier onset of the fall cholera season, which suggests that flooding may not only increase cholera attack rates but also hasten the postmonsoon epidemic peak. Statistical evidence for a seasonal shift is limited, however, by the low number of extreme events in these data.

Importantly, the remote forcing of Dhaka cholera by SST in the Pacific at a relatively long lead time (11 mo) affords an opportunity for anticipating outbreaks using model-based forecasts. To assess our model's prediction performance, we took a cross-validation approach, sequentially removing 1 y of data, refitting the model to the remaining data, and then simulating 11 mo into the future to assess forecasting accuracy. Fig. 4 shows that the predicted rate of cases is highly coherent with the observed rate. We checked that the model fulfills the basic requirement for forecasting skill, namely that it outperforms the simpler model given by the seasonal means (25); our model's 11-mo predictions' sum of squared error (SSE) is 79% that of the seasonal mean model. When we remove months of the year with consistently low cholera (December through March), our model's SSE is 75% that of the seasonal model. We also considered a more stringent benchmark based on ENSO. Specifically, we adjusted the seasonal prediction according to the linear relationship between ENSO and the cholera anomaly. Not surprisingly, this benchmark improves on the strictly seasonal model: Its SSE is 84% of that of the seasonal mean model. Our model outperforms the stricter benchmark, with an SSE 12% smaller during months when cholera is present.

More relevant to public health is the model's skill at predicting the chance of a large outbreak. We evaluated the performance of our model at this task. Specifically, we used the model to predict the chance of monthly cholera incidence exceeding its 75th percentile in 11 mo. Thus, for example, Fig. 4, *Left Inset* shows the distribution of model forecasts for October 1998 based on November 1997 data. Although the mean prediction differs from the observation, almost all (>99%) model simulations resulted in large events. Thus, our model would have, with high confidence, predicted a large outbreak in October 1998 due to the large preceding El Niño event. Fig. 4, *Right Inset* repeats this hindsight analysis for May 2003 (using data from June 2002). Here, we find a reduced, but still large (~87%) probability of large outbreak. By construction, our model tends to underestimate the size of outbreaks: We find that an outbreak probability >26% (and not 50%) should be interpreted as an indication of risk (see *section S5* and Figs. S6 and S7).

Using the 75th percentile definition of a large event, we find false positive and false negative rates of ~25%, but that the chance of observing an outbreak when none is predicted is only 10% (10/99 mo). *Section S6* contains further discussion of our probabilistic forecasts and their interpretation.

An 11-mo lead time makes a cholera early-warning system based on the MDIMC model and ENSO practically operational. A short lead-time model with an accurate flooding index would

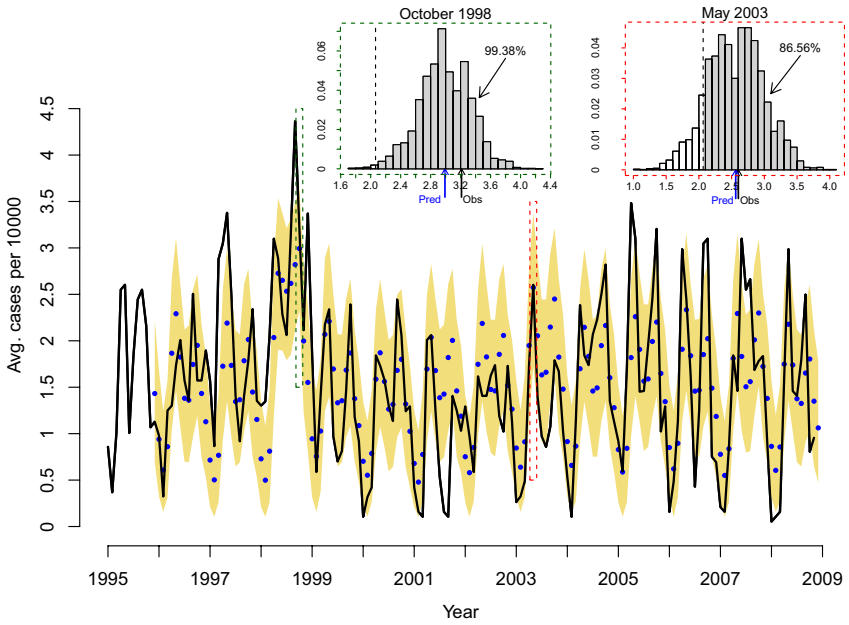

Fig. 4. Eleven-month predictions (blue dots) with empirical estimate of 95% confidence interval (yellow shaded region) vs. the observed data (black line). (*Left Inset*) Distribution of predictions for October 1998. (*Right Inset*) Distribution of predictions for May 2003.

allow updating of 11-mo predictions immediately before and during the postmonsoon season.

Because it is annualized, the flooding index considered here is of limited practical application to prediction. However, because most of the flooding occurs during the monsoon season, this index is well correlated with cholera throughout the city in the monsoon season ($r = 0.91$; Fig. S8). Our results suggest that a complementary short lead-time model based on an accurate monthly flooding index would allow updating of long-range predictions 1–2 mo before the onset of the postmonsoon cholera season. The evidence that the effect of flooding on cholera is fully felt only 4–7 wk after initial flooding (23) further supports this suggestion. Our results suggest too that efforts to forecast flooding itself are likely to prove valuable for cholera early warning.

Because our modeling framework permits assessment of the effects of spatial and temporal variables on disease in a straightforward and effective way, it should prove useful for investigations of other diseases in other large cities. It complements previous approaches to the larger-scale spatiotemporal dynamics of infectious diseases inspired by metapopulation models in ecology (26, 27). Indeed, the approach described here can be viewed as an extension of presence/absence models (26) to more than two states. As with the earlier approaches, the MDIMC framework is simple, flexible, and straightforward to fit by maximum likelihood. The likelihood-ratio test affords a convenient means of discounting model complexity. Our modeling framework also complements more recent efforts to model the detailed spatial spread of cholera in Haiti at the shorter timescales of an individual outbreak following the introduction of the disease into a fully susceptible population (28–30). Models incorporating spatial effects of "gravity" type have proved useful in this context (31, 32); their utility in the context of urban and endemic cholera remains to be seen. More generally, spatial structures more complex than the nearest-neighbor effect we have considered here can be incorporated and tested within the MDIMC framework. On another front, we are currently exploring more systematic methods of identifying spatial heterogeneities of the type described here. Specifically, we are developing statistical approaches for the objective identification of regions sharing similar dynamics. Although more sophisticated models yielding more skillful predictions are without doubt possible for cholera, our results—the most skillful forecasts to date at lead times of practical utility—make unequivocally clear that such forecasts must account appropriately for heterogeneities at local scales.

Interestingly we found that the action of the global driver, ENSO, on cholera in Dhaka is locally differentiated: The sensitive city core acts to couple climate variability to interannual variation of disease and propagates the risk of disease to the rest of the city. The partition of the city into two dynamically distinct regions maps well onto the distribution of demographic parameters closely linked to socioeconomic conditions: The core districts are largely those with the highest population density, the highest number of the poorest kind of housing, and the greatest reliance on municipal tap water (as opposed to wells; Fig. S9). The existence of a sensitive core is consistent, too, with the well-established roles of sanitary conditions and access to clean water as key risk factors for a fecal–oral disease such as cholera. For these reasons, we hypothesize that the flooding-induced breakdown of sanitary conditions is likely the principal mediator of the effect of climate on the postmonsoon peak in the core districts of Dhaka. More generally, our results show that spatial structure within a city is central not only in the fine-scale structure of transmission classically illustrated by Snow's famous map of London's 1854 cholera epidemic (19), but also to the disease's dynamical response to climate forcing at the megacity scale.

ACKNOWLEDGMENTS. We thank Benjamin A. Cash for his input on climate data, and Andrea Rinaldi and two anonymous referees for helpful comments. This research was supported by the National Oceanic and Atmospheric Administration's Program on Oceans and Health (Grant # F020704). The cholera case data used in this paper were collected with the support of ICDDR,B and its donors who provide unrestricted support to ICDDR,B for its operation and research. Current donors providing unrestricted support include the Government of the People's Republic of Bangladesh, the Canadian International Development Agency, the Swedish International Development Cooperative Agency, and the Department for International Development, United Kingdom. We gratefully acknowledge these donors for their support and commitment to ICDDR,B's research efforts. M.P. is an investigator of the Howard Hughes Medical Institute. A.A.K. acknowledges the support of the Research and Policy for Infectious Disease Dynamics program of the Science and Technology Directorate, Department of Homeland Security, and the Fogarty International Center, National Institutes of Health.

1. Longini IM, Jr., et al. (2002) Epidemic and endemic cholera trends over a 33-year period in Bangladesh. *J Infect Dis* 186:246–251.
2. Koelle K, Rodó X, Pascual M, Yunus M, Mostafa G (2005) Refractory periods and climate forcing in cholera dynamics. *Nature* 436:696–700.
3. Glass RI, et al. (1982) Endemic cholera in rural Bangladesh, 1966-1980. *Am J Epidemiol* 116:959–970.
4. Pascual M, Rodó X, Ellner SP, Colwell R, Bouma MJ (2000) Cholera dynamics and El Nino-southern oscillation. *Science* 289:1766–1769.
5. Lobitz B, et al. (2000) Climate and infectious disease: Use of remote sensing for detection of Vibrio cholerae by indirect measurement. *Proc Natl Acad Sci USA* 97:1438–1443.
6. Constantin de Magny G, et al. (2008) Environmental signatures associated with cholera epidemics. *Proc Natl Acad Sci USA* 105:17676–17681.
7. Matsuda F, et al. (2007) Prediction of epidemic cholera due to vibrio cholerae o1 in children younger than 10 years using climate data in bangladesh. *Epidemiol Infect* 136:1–7.
8. Rodo X, Pascual M, Fuchs G, Faruque ASG (2002) ENSO and cholera: A nonstationary link related to climate change? *Proc Natl Acad Sci USA* 99:12901–12906.
9. Hashizume M, et al. (2008) The effect of rainfall on the incidence of cholera in Bangladesh. *Epidemiology* 19:103–110.
10. Moran P (1953) The statistical analysis of the Canadian lynx cycle. 1. Structure and prediction. *Aust J Zool* 1:163–173.
11. Hudson PJ, Cattadori IM (1999) The Moran effect: A cause of population synchrony. *Trends Ecol Evol* 14:1–2.
12. Lipp EK, Huq A, Colwell RR (2002) Effects of global climate on infectious disease: The cholera model. *Clin Microbiol Rev* 15:757–770.
13. Sack RB, et al. (2003) A 4-year study of the epidemiology of *Vibrio cholerae* in four rural areas of Bangladesh. *J Infect Dis* 187:96–101.
14. Pascual M, Bouma MJ, Dobson AP (2002) Cholera and climate: Revisiting the quantitative evidence. *Microbes Infect* 4:237–245.
15. Cash B, Rodó X, Kinter J (2008) Links between tropical Pacific SST and cholera incidence in Bangladesh: Role of the Eastern and Central tropical Pacific. *J Climate* 21: 4647–4663.
16. Cash B, Rodó X, Kinter J, III (2008) Links between tropical Pacific SST and cholera incidence in Bangladesh: Role of the eastern and central tropical Pacific. *J Clim* 21: 4647–4663.
17. Bugliarello G (1999) Megacities and the developing world. *BRIDGE Wash.* 29:19–26.
18. Marshall J (2005) Environmental health: Megacity, mega mess.... *Nature* 437:312–314.
19. Snow J (1855) *On the Mode of Communication of Cholera,* (J. Churchill, London), 2nd Ed.
20. Caswell H, Cohen J (1991) Disturbance, interspecific interaction and diversity in metapopulations. *Biol J Linn Soc Lond* 42:193–218.
21. Caswell H (2001) *Matrix Population Models* (Sinauer, Sunderland, MA).
22. Akanda A, Jutla A, Islam S (2009) Dual peak cholera transmission in Bengal Delta: A hydroclimatological explanation. *Geophys Res Lett* 36:L19401.
23. Schwartz BS, et al. (2006) Diarrheal epidemics in Dhaka, Bangladesh, during three consecutive floods: 1988, 1998, and 2004. *Am J Trop Med Hyg* 74:1067–1073.
24. Harris A, et al. (2008) Shifting prevalence of major diarrheal pathogens in patients seeking hospital care during floods in 1998, 2004, and 2007 in Dhaka, Bangladesh. *Am J Trop Med Hyg* 79:708–714.
25. Shukla J (2007) Atmosphere. Monsoon mysteries. *Science* 318:204–205.
26. Hanski I (1999) *Metapopulation Ecology* (Oxford Univ Press, New York).
27. Xia Y, Bjørnstad ON, Grenfell BT (2004) Measles metapopulation dynamics: A gravity model for epidemiological coupling and dynamics. *Am Nat* 164:267–281.
28. Bertuzzo E, et al. (2011) Prediction of the spatial evolution and effects of control measures for the unfolding Haiti cholera outbreak. *Geophys Res Lett* 38:L06403.
29. Tuite AR, et al. (2011) Cholera epidemic in Haiti, 2010: Using a transmission model to explain spatial spread of disease and identify optimal control interventions. *Ann Intern Med* 154:593–601.
30. Chao DL, Halloran ME, Longini IM, Jr. (2011) Vaccination strategies for epidemic cholera in Haiti with implications for the developing world. *Proc Natl Acad Sci USA* 108:7081–7085.
31. Ferrari MJ, et al. (2008) The dynamics of measles in sub-Saharan Africa. *Nature* 451: 679–684.
32. Eggo RM, Cauchemez S, Ferguson NM (2011) Spatial dynamics of the 1918 influenza pandemic in England, Wales and the United States. *J R Soc Interface* 8:233–243.